THE ASTROPHYSICAL JOURNAL, 482:L131–L134, 1997 June 20

THE TEMPERATURE OF EXTENDED GAS IN ACTIVE GALAXIES: EVIDENCE FOR MATTER-BOUNDED CLOUDS

A. S. WILSON[1,2]
Space Telescope Science Institute, 3700 San Martin Drive, Baltimore, MD 21218

AND

L. BINETTE[3] AND T. STORCHI-BERGMANN[2]
Instituto de Física, Universidade Federal do Rio Grande do Sul, Campus do Vale, C.P. 15051, 91501-970 Porto Alegre, RS, Brazil
Received 1997 January 27; accepted 1997 March 31

ABSTRACT

We report measurements of the electron temperature at about a dozen locations in the extended emission-line regions of five active (Seyfert and radio) galaxies. Temperatures ($T_{[O\,III]}$ and $T_{[N\,II]}$) have been determined from both the $I([O\,III]\ \lambda4363)/I([O\,III]\ \lambda5007)$ and $I([N\,II]\ \lambda5755)/I([N\,II]\ \lambda6583)$ ratios. $T_{[O\,III]}$ lies in the range (1.0–1.7) $\times$ 10^4 K. We find a strong trend for $T_{[O\,III]}$ to be higher than $T_{[N\,II]}$, with the difference typically being $\approx$5000 K. Because the critical density for collisional de-excitation of the $^1D_2$ level in N II is lower than that of the same level in O III, the deviations of the measured intensity ratios from those expected for $T_{[O\,III]} = T_{[N\,II]}$ in the low-density limit are unlikely to result from collisional de-excitation. The measured values of $T_{[O\,III]}$ and the differences between $T_{[O\,III]}$ and $T_{[N\,II]}$ are very similar to those found in Galactic planetary nebulae. It is argued that the dominant form of energy input to the clouds is photoionization, but detailed modeling indicates that the temperature difference is too large to be accounted for in terms of photoionization of ionization-bounded clouds. We propose instead that both matter- and ionization-bounded clouds are present in the extended emission-line regions, with most of the [O III] emission originating from a hot zone in the matter-bounded clouds and essentially all the [N II] from the ionization-bounded clouds.

Subject headings: galaxies: active — galaxies: ISM — galaxies: nuclei — galaxies: Seyfert — line: formation — radio continuum: galaxies

1. INTRODUCTION

High-ionization narrow emission lines are a defining characteristic of the nuclei of Seyfert galaxies and are often seen in radio galaxies. The gas emitting these lines is generally believed to be photoionized, though the origin of the ionizing photons is still debated. Spectroscopic studies have focused mostly on the spatially unresolved nuclei, the narrow-line emission of which originates from gas with a wide range of densities (10^2 cm^{-3} $\leq n_e \leq$ 10^7 cm^{-3}). This large spread of densities, together with the unknown distances of the individual gas clouds from the source of ionizing photons, leads to serious ambiguities in photoionization models. For example, collisional de-excitation of the $^1D_2$ level of O III becomes significant for $n_e \geq 10^5$ cm^{-3}, rendering the intensity ratio $R_{[O\,III]} = I(\lambda4363)/I(\lambda5007)$ an unreliable measure of electron temperature (Osterbrock 1989).

The high-ionization gas is, however, often spatially extended in ground-based observations of both Seyfert (e.g., Mulchaey, Wilson, & Tsvetanov 1996) and radio (e.g., Baum & Heckman 1989) galaxies. Study of such extended gas provides two advantages. First, the density is low ($n_e \leq 10^3$ cm^{-3}; see, e.g., Morganti et al. 1991; Tadhunter, Metz, & Robinson 1994), so that collisional de-excitation is unimportant for most forbidden lines, the exceptions providing density diagnostics. Second, the geometric properties of the gas, including its distance from the nucleus, can be measured directly. These extended emission-line regions (EELRs) thus provide much simpler physical situations than the spatially unresolved narrow- or broad-line regions, and their excitation should be correspondingly easier to understand.

Tadhunter, Robinson, & Morganti (1989) have presented measurements of $R_{[O\,III]}$ for 12 locations in EELRs around six active galaxies. These measurements imply electron temperatures in the range 12,800 K $< T_{[O\,III]} <$ 22,000 K, whereas photoionization models that successfully account for most other line ratios predict $T_{[O\,III]} <$ 11,000 K. These high measured temperatures were confirmed by Storchi-Bergmann et al. (1996), who found 10,000 K $< T_{[O\,III]} <$ 17,000 K for EELRs around five active (both Seyfert and radio) galaxies. Tadhunter et al. (1989) concluded that either the EELRs have a heating source in addition to photoionization—plausibly cosmic rays or shocks—or the metal abundances are lower than the solar values assumed in the models. Binette, Wilson, & Storchi-Bergmann (1996, hereafter BWSB) favored an alternative picture in which there are two populations of ionized clouds—a matter-bounded (MB) component responsible for most of the He II and high-ionization forbidden-line emission, and an ionization-bounded (IB) component emitting low- to intermediate-ionization forbidden lines. In this model, the IB clouds are illuminated by an ionizing continuum modified by absorption in the MB clouds. A new sequence of photoionization models was thereby obtained by varying the ratio, $A_{M/I}$, of the solid angle subtended by the MB clouds at the ionizing source to that subtended by the IB clouds. The main success of the $A_{M/I}$ sequence of models is that it provides a natural

[1] Also Department of Astronomy, University of Maryland, College Park, MD 20742.

[2] Visiting Astronomer, Cerro Tololo Inter-American Observatory, operated by the Association of Universities for Research in Astronomy, Inc., under contract with the National Science Foundation.

[3] Also European Southern Observatory, Casilla 19001, Santiago 19, Chile.

explanation for observed correlations between both the I([Ne V] λ3426)/I([O II] λλ3727) and I([O III] λ5007)/I([O II] λλ3727) ratios and the I(He II λ4686)/I(Hβ) ratio (BWSB). Such a correlation between the gaseous ionization, measured from the forbidden lines, and the I(He II λ4686)/I(Hβ) ratio cannot be understood in terms of the standard U (ionization parameter) sequence, since the He II λ4686/Hβ ratio for IB clouds depends primarily upon the slope of the ionizing continuum between 13.6 and 54.4 eV and is relatively insensitive to U. Further, the electron temperature $T_{[O\,III]}$ is correctly predicted by the $A_{M/I}$ sequence, provided the thickness and ionization parameter of the MB component are appropriately selected. Finally, much stronger high-ionization lines (e.g., [Ne V] λ3426 and C IV λλ1549) are expected in the $A_{M/I}$ sequence than in the U sequence, again in accord with observations.

In the $A_{M/I}$ sequence, the [O III] λ5007 and λ4363 emission originates mostly in the MB clouds, while essentially all [N II] λ6583 and λ5755 emission comes from the IB clouds. Because the MB clouds are hotter than the IB ones (see Figs. 1 and 2 of BWSB), the temperature $T_{[O\,III]}$ inferred from $R_{[O\,III]}$ should be considerably greater than the temperature $T_{[N\,II]}$ inferred from $R_{[N\,II]} = I(\lambda5755)/I(\lambda6583)$. BWSB predicted that $T_{[O\,III]}$ should be ≃5000 K greater than $T_{[N\,II]}$ in the $A_{M/I}$ sequence, but only slightly higher (by less than 1000 K) in the U sequence. The temperature $T_{[N\,II]}$ is predicted to be 9200 K for solar abundances in the $A_{M/I}$ sequence, given the value of U assumed by BWSB for the IB clouds. These predictions of the $A_{M/I}$ sequence models are in good agreement with temperature measurements of the northwest cloud of Cygnus A, which give $T_{[O\,III]} = 15{,}000 \pm 1000$ K and $T_{[N\,II]} = 10{,}000 \pm 600$ K (Tadhunter et al. 1994).

In a typical Seyfert galaxy, I([O III] λ5007)/I(Hβ) ≃ 10, I(Hα)/I(Hβ) ≃ 3, and I([N II] λ6583)/I(Hα) ≃ 1. For $T_e = 10^4$ K, $R_{[N\,II]} = 0.016$ and $R_{[O\,III]} = 0.0064$ (Osterbrock 1989). Thus, if $T_{[N\,II]} = T_{[O\,III]} = 10^4$K, [N II] λ5755 and [O III] λ4363 should have roughly the same strength [I([O III] λ4363) ≃ 1.3I([N II] λ5755)] and be about equally easy to detect with modern CCD spectrographs. However, this expectation is not borne out by our observations.

The purpose of the present Letter is to provide further measurements of $T_{[N\,II]}$ in EELRs and to evaluate the implications for the gaseous excitation. We find a strong tendency for $T_{[O\,III]}$ to exceed $T_{[N\,II]}$ by several thousand kelvins and note that a similar trend, with a similar range of temperatures, is found in Galactic planetary nebulae. It is argued that the most likely explanation is that the EELRs contain both matter- and ionization-bounded clouds.

2. RESULTS

In their study of nuclear and EELR spectra of five active galaxies, Storchi-Bergmann et al. (1996) reported a detection of [N II] λ5755 at only one location—the nucleus of Mrk 573. We have, therefore, measured upper limits on the flux of this line at the 12 other locations where Storchi-Bergmann et al. obtained spectra. Two methods were used. In the first, a spectrally unresolved artificial line was superposed on the continuum and its flux adjusted by eye to provide an upper limit to the actual line flux. In the second method, the formal rms noise in the continuum was calculated, and the 3 × rms upper limit on the flux of an unresolved spectral line was determined. In some cases, the upper limits for these two approaches agreed quite well, while in others the first method yielded a higher value. We decided to adopt the more conservative upper limits from the first method.

One concern was that the stellar template spectrum (which was subtracted from the observed spectrum prior to measuring the emission lines; see Storchi-Bergmann et al. 1996) might, for some unknown reason, be a poor match near the λ5755 rest wavelength. If the template were too high, a real emission line could have been mistakenly subtracted away. Examination of the two templates used by Storchi-Bergmann et al. showed them to be in excellent agreement in the spectral region in question and that λ5755 corresponds to a local minimum. Since the templates match the stellar continuum very well almost everywhere else, we have no reason to doubt the validity of the template subtraction.

The resulting upper limits to [N II] λ5755, and the fluxes of [N II] λ6583, [O III] λ4363, and [O III] λ5007, were corrected for obscuration, when present, using Storchi-Bergman et al.'s values of A_V, which were obtained under the assumption of an intrinsic emission-line Balmer decrement of Hα/Hβ = 3.1. Correction for obscuration was not possible for the nucleus of ESO 362−G8, because a reliable measurement of Hβ could not be obtained, as a result of the A-type stellar continuum; the nucleus of this galaxy is omitted from the following discussion. The measurements of or limits on $R_{[N\,II]}$ and $R_{[O\,III]}$ were then converted to $T_{[N\,II]}$ and $T_{[O\,III]}$ by using equations (5.5) and (5.4) of Osterbrock (1989), respectively, assuming the low-density limit.

The results are shown in the left panel of Figure 1, in which $T_{[O\,III]}$ is plotted against $T_{[N\,II]}$. It is immediately apparent that $T_{[O\,III]}$ tends to be greater than $T_{[N\,II]}$ by an amount that ranges up to ≈7000 K but is more typically ≈5000 K. This trend is found for the nucleus of NGC 526A and for most of the off-nuclear locations (only upper limits to both temperatures are available for the nuclei of PKS 0349−278 and PKS 0624−206). It is unlikely that this trend is related to collisional de-excitation of the $^1D_2$ levels, since (1) the critical densities of 8.6×10^4 cm^{-3} (for N II) and 7.0×10^5 cm^{-3} (for O III) are much higher than expected for off-nuclear gas and (2) such collisional de-excitation effects would tend to depress [N II] λ6583 at a lower density than [O III] λ5007, thus *increasing* $R_{[N\,II]}$ and the calculated value of $T_{[N\,II]}$ relative to $R_{[O\,III]}$ and $T_{[O\,III]}$.

The right panel of Figure 1 shows a similar plot for Galactic planetary nebulae, using the measurements of Kingsburgh & Barlow (1994). The range of [O III] temperatures is similar to that seen in the active galactic nuclei (AGNs), and there is also a trend for $T_{[O\,III]}$ to exceed $T_{[N\,II]}$ (see also Torres-Peimbert & Peimbert 1977; Kaler 1986). The trends between $T_{[O\,III]}$ and $T_{[N\,II]}$ in planetary nebulae are generally considered to be excitation effects in a photoionized gas (Kaler 1986). The similar behavior of the AGN EELRs then strongly suggests that the same may be true for them.

3. DISCUSSION

The photoionization code MAPPINGS IC (Binette et al. 1993; Ferruit et al. 1997) has been used to calculate the expected values of $R_{[O\,III]}$ and $R_{[N\,II]}$ in various situations. We began by considering IB, isobaric, dust-free ($\mu = 0$)[4] clouds of

[4] Here μ is the dust-to-gas ratio of the cloud in units of the solar neighborhood dust-to-gas ratio.

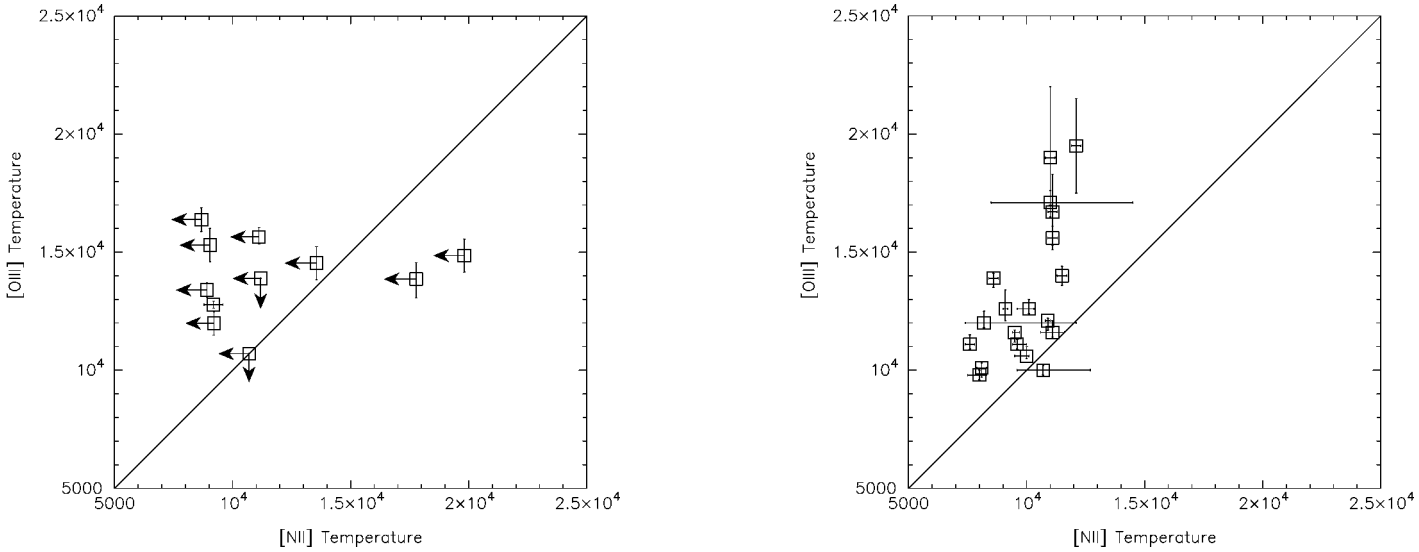

FIG. 1.—*Left*: [O III] temperature vs. [N II] temperature (in kelvins) for nuclear and extended gas in active galaxies. Temperatures are plotted for all locations at which spectra were obtained by Storchi-Bergmann et al. (1996), except for the nucleus of ESO 362−G8 (see text) and 10″ northwest of the nucleus of PKS 0634−206, at which only a poor upper limit on $T_{[N\,II]}$ could be obtained. The error bars are dominated by the uncertainties in the fluxes of [O III] λ4363 and [N II] λ5755. The straight line represents $T_{[O\,III]} = T_{[N\,II]}$. The temperature-sensitive line [N II] λ5755 is detected in only the nucleus of Mrk 573, so the [N II] temperatures are upper limits at all other positions. *Right*: A similar plot for planetary nebulae, constructed from the temperatures and their errors listed by Kingsburgh & Barlow (1994). It is notable that the range of $T_{[O\,III]}$ is similar in the two types of object and that there is a trend for $T_{[O\,III]} > T_{[N\,II]}$ in both types.

solar metallicity ($Z = 1$) and low density ($n = 1000$ cm^{-3} at the irradiated face) photoionized by continua of various shapes—blackbodies, power laws, and a spectrum with a UV bump. A grid of models was generated by varying the ionization parameter U. The results are plotted in Figure 2, in which the models represented by the long-dashed (power-law ionizing spectrum) and solid (blackbody ionizing spectrum) lines have [O III] λ5007/H$\beta \leq 16$, and are thus consistent with the observed values of this ratio, while the dotted extensions have [O III] λ5007/H$\beta > 16$ and are thus unacceptable. The models with [O III] λ5007/H$\beta \leq 16$ do show deviations from the $T_{[O\,III]} = T_{[N\,II]}$ line, but these differences between $T_{[O\,III]}$ and $T_{[N\,II]}$ are much smaller than are observed. A power-law model with very low metallicity ($Z = 0.2$) provides [O III] temperatures in general agreement with those observed, even without dust ($\mu = 0$), but again the difference between $T_{[O\,III]}$ and $T_{[N\,II]}$ is too small. In addition, such a low metallicity is implausible for the circumnuclear emission-line regions discussed here. A high-density ($n = 60{,}000$ cm^{-3}) model lies to the right of the $T_{[O\,III]} = T_{[N\,II]}$ line, confirming that collisional de-excitation tends to *increase* $R_{[N\,II]}$ relative to $R_{[O\,III]}$, which is opposite to the trend observed.

As a second step, we have considered MB clouds. We adopt the model of BWSB, which contains two cloud populations—high-ionization MB clouds and low-ionization IB clouds. The two vertical dashed lines in Figure 2 show the predicted behavior of $R_{[O\,III]}$ and $R_{[N\,II]}$ as a function of the parameter $A_{M/I}$ (defined in § 1). The model marked "$A_{M/I}$ $\alpha = -1.3$" is the same as that described in BWSB and represents a varying proportion of MB clouds (with $U_{MB} = 0.04$) and IB clouds (with $U_{IB} = 5.2 \times 10^{-4}$). The model marked "$A_{M/I}$ $\alpha = -1.1$" has a harder continuum, $U_{MB} = 0.03$, and $U_{IB} = 1.8 \times 10^{-4}$. The predictions of these models are in agreement with the measured values in the nucleus of Mrk 573 and in the northwest cloud of Cyg A and are consistent with most of the other points. These models were also shown by BWSB to be in agreement with the other optical line ratios. It should be emphasized that our models assume a single ionization parameter and total column for each of the matter- and ionization-bounded populations of clouds, which represents a gross oversimplification of a probably complex situation involving a continuous range of U_{MB}, U_{IB}, and the column density through the clouds. The model predictions should thus be considered as illustrative rather than definitive. Nevertheless, the key prediction (BWSB) of the matter- plus ionization-bounded model—that $T_{[O\,III]}$ should exceed $T_{[N\,II]}$ by ≈5000 K—seems to be borne out by the data.

Potential sources of uncertainty are noncollisional contributions to [O III] λ4363. Such contributors include charge transfer (see, e.g., Dalgarno & Sternberg 1982) and recombination (see, e.g., Rubin 1986). The relative contribution of these effects is lower at higher temperatures because of the exponential temperature dependence of collisional excitation. Although no detailed calculations are available in the AGN context, and population of the $^1S_0$ level of O III by these processes is not included in MAPPINGS IC, we infer from calculations with hot stellar ionizing sources (Kingdon & Ferland 1995) that the resulting error is less than 300 K when $T_{[O\,III]} > 10{,}000$ K. Therefore, recombination processes make a very minor contribution to [O III] λ4363 in the AGN context.

Last, there is the question whether sources of energy other than photoionization may contribute to the temperature difference between [O III] and [N II]. Such sources include shocks, which may be generated by outflowing winds or jets, and relativistic particles. While temperature stratification is expected in classical shock models (e.g., Binette, Dopita, & Tuohy 1985), it is important to emphasize that the line ratios seen in the extended emission-line regions under study are characteristic of photoionization by a hard spectrum (BWSB). Shocks with photoionized precursors can generate spectra that

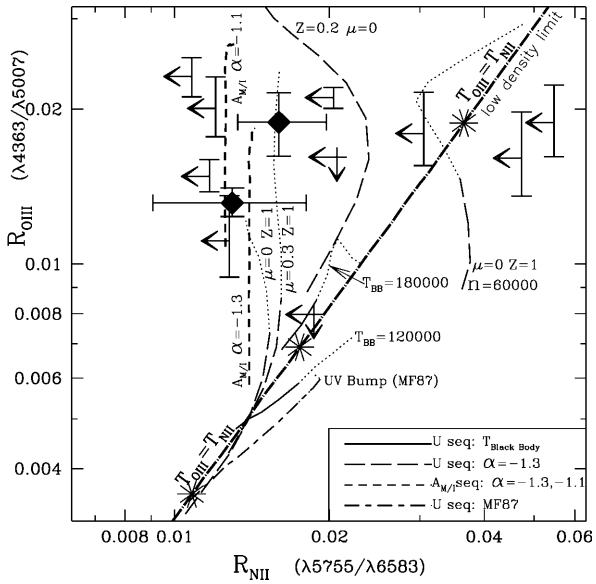

FIG. 2.—$R_{[O\,III]} = I(\lambda4363)/I(\lambda5007)$ vs. $R_{[N\,II]} = I(\lambda5755)/I(\lambda6583)$. Diamonds represent the measured ratios in the nuclei of Mrk 573 and the northwest cloud of Cyg A (Tadhunter et al. 1994), while the error bars and upper limits represent our other measurements (see Fig. 1). The straight dot-dashed line is the locus $T_{[O\,III]} = T_{[N\,II]}$ in the low-density limit; the three asterisks represent temperatures of 8500, 10,000, and 15,000 K (from lower left to upper right). All other lines represent model predictions calculated with MAPPINGS IC. Unless otherwise noted, the models are for ionization-bounded, dust-free, isobaric clouds of solar abundance and density 1000 cm^{-3}. The two solid lines are sequences of ionization parameter with a blackbody ionizing continuum having the temperatures indicated. For these models represented by the solid lines, the ratio [O III] $\lambda5007/H\beta \leq 16$, in accord with observations. The dotted extensions to the solid lines have [O III] $\lambda5007/H\beta > 16$. The four long-dashed lines are sequences of ionization parameter for ionization-bounded clouds, with indicated abundance (Z) and dust content (μ), ionized by a power-law ionizing continuum of index $\alpha = -1.3$. These four models have [O III] $\lambda5007/H\beta \leq 16$ where the line is long-dashed, but [O III] $\lambda5007/H\beta > 16$ for the dotted extensions. The long-dashed curve to the right is for high-density (60,000 cm^{-3}) clouds. The long-dash–short-dashed line toward the bottom is a sequence of ionization parameter for a broken power law ionizing spectrum (simulating a UV bump), following Mathews & Ferland (1987). Last, the two vertical short-dashed lines to the left are models of the $A_{M/I}$ sequence with $Z = 1$, $\mu = 0.015$, and power-law ionizing continua of index $\alpha = -1.3$ and $\alpha = -1.1$. The parameter $A_{M/I}$ increases from 0.04 at the bottom to 16 at the top.

resemble those of Seyfert galaxies (Dopita & Sutherland 1995), but then the temperature is expected to be similar to that found in classical photoionization models of IB clouds (see Fig. 7 of Dopita & Sutherland 1995). Relativistic particles may contribute heating (Ferland & Mushotzky 1984), but most of the off-nuclear regions that we have studied do not have strong radio emission. Also, it is unclear why the relativistic particles would heat the O III region preferentially over the N II.

In summary, the range of electron temperature and the difference between $T_{[O\,III]}$ and $T_{[N\,II]}$ are very similar in planetary nebulae and the EELRs of active galaxies. These similarities do not favor a major contribution to the temperature from shock heating in the galaxies, despite the higher gas velocities there. More generally, the similarities between the two classes of objects support the idea that the difference between the [O III] and [N II] temperatures is primarily related to the structure of the ionized clouds, rather than the presence of extra heating sources or a property of the ionizing source. Indeed, the presence of matter-bounded clouds in some planetary nebulae is demonstrated by differences between the two Zanstra temperatures derived from the nebular H I and He II lines (Osterbrock 1989, p. 150) and also possibly by discrepancies between the Zanstra temperatures and the spectroscopic effective temperature of the central star (see, e.g., Kudritzki & Méndez 1989).

A. S. W. thanks J. P. Harrington for several valuable discussions. This research was supported in part by NASA under grants NAGW-4700 and NAG 8-1027 and by the Space Telescope Science Institute through grants GO-5411 and GO-6006. L. B. is grateful to CNPq and CAPES of Brazil for financial assistance.

REFERENCES

Baum, S. A., & Heckman, T. M. 1989, ApJ, 336, 681
Binette, L., Dopita, M. A., & Tuohy, I. R. 1985, ApJ, 297, 476
Binette, L., Wang, J. C. L., Zuo, L., & Magris, C. M. 1993, AJ, 105, 797
Binette, L., Wilson, A. S., & Storchi-Bergmann, T. 1996, A&A, 312, 365 (BWSB)
Dalgarno, A., & Sternberg, A. 1982, ApJ, 257, L87
Dopita, M. A., & Sutherland, R. S. 1995, ApJ, 455, 468
Ferland, G. J., & Mushotzky, R. F. 1984, ApJ, 286, 42
Ferruit, P., Binette, L., Sutherland, R. S., & Pécontal, E. 1997, A&A, in press
Kaler, J. B. 1986, ApJ, 308, 322
Kingdon, J. B., & Ferland, G. J. 1995, ApJ, 450, 691
Kingsburgh, R. L., & Barlow, M. J. 1994, MNRAS, 271, 257
Kudritzki, R.-P., & Méndez, R. H. 1989, in IAU Symp. 131, Planetary Nebulae, ed. S. Torres-Peimbert (Dordrecht: Kluwer), 273
Mathews, W. G., & Ferland, G. J. 1987, ApJ, 323, 456
Morganti, R., Robinson, A., Fosbury, R. A. E., di Serego Alighieri, S., Tadhunter, C. N., & Malin, D. F. 1991, MNRAS, 249, 91
Mulchaey, J. S., Wilson, A. S., & Tsvetanov, Z. 1996, ApJS, 102, 309
Osterbrock, D. E. 1989, Astrophysics of Gaseous Nebulae and Active Galactic Nuclei (Mill Valley, CA: Univ. Sci.)
Rubin, R. H. 1986, ApJ, 309, 334
Storchi-Bergmann, T., Wilson, A. S., Mulchaey, J. S., & Binette, L. 1996, A&A, 312, 357
Tadhunter, C. N., Metz, S., & Robinson, A. 1994, MNRAS, 268, 989
Tadhunter, C. N., Robinson, A., & Morganti, R. 1989, in ESO Workshop on Extranuclear Activity in Galaxies, ed. E. J. A. Meurs & R. A. E. Fosbury (Garching: ESO), 293
Torres-Peimbert, S., & Peimbert, M. 1977, Rev. Mexicana Astron. Astrofis., 2, 181